

Review

- R15 Neurobiological bases of spatial learning in the natural environment: neurogenesis and growth in the avian and mammalian hippocampus
D. W. Lee, L. E. Miyasato and N. S. Clayton

Research papers

- 1261 Neuromagnetic activity in the human left cerebral hemisphere concerning logical processing during auditory oddball stimulation
H. Yoshida, M. Iwahashi, M. Yamaguchi and M. Tonoike
- 1267 Novel splice variants of the voltage-sensitive sodium channel alpha subunit
Y. Oh and S. G. Waxman
- 1273 Sublethal in vitro glucose-oxygen deprivation protects cultured hippocampal neurons against a subsequent severe insult
L. Khaspekov, M. Shamloo, I. Victorov and T. Wieloch
- 1277 Protection by pyruvate and malate against glutamate-mediated neurotoxicity
F. Ruiz, G. Alvarez, R. Pereira, M. Hernández, M. Villalba, F. Cruz, S. Cerdán, E. Bogóñez and J. Satrustegui
- 1283 Effects of 18-methoxycoronaridine on acute signs of morphine withdrawal in rats
B. Rho and S. D. Glick
- 1287 Neuroprotective effects of a novel AMPA receptor antagonist, YM872
D. L. Small, C. L. Murray, R. Monette, S. Kawasaki-Yatsugi and P. Morley
- 1291 Polymorphism in the promoter region of the α_{2A} adrenergic receptor gene and mood disorders
K. Ohara, M. Nagai, K. Tani, T. Tsukamoto, Y. Suzuki and K. Ohara
- 1295 5'-Heterogeneity of the human excitatory amino acid transporter cDNA EAAT2 (GLT-1)
C. Münch, B. Schwalenstöcker, B. Knappenberger, S. Liebau, H. Völkel, A. C. Ludolph and T. Meyer
- 1299 Diffusion heterogeneity and anisotropy in rat hippocampus
T. Mazel, Z. Šimonová and E. Syková
- 1305 Low activity allele of catechol-o-methyltransferase gene and Japanese unipolar depression
K. Ohara, M. Nagai, Y. Suzuki and K. Ohara
- 1309 Localization of Ca-ATPase in frog crista ampullaris
L. Gioglio, G. Russo, W. Marcotti and I. Prigioni
- 1313 MK-801 does not enhance dopaminergic cell survival in embryonic nigral grafts
G. S. Schierle, J. Karlsson and P. Brundin
- 1317 Differences in the cerebrovascular anatomy of C57Black/6 and SV129 mice
K. Maeda, R. Hata and K.-A. Hossmann
- 1321 Influence of stimulus speed upon the antagonistic surrounds of area MT/V5 neurons
D.-K. Xiao, S. Raiguel, V. Marcar and G. A. Orban
- 1327 Microdialysis and EEG in rats reveal cortical PGE2 changes during sleep and wakefulness
K. Gerozissis, Z. de Saint-Hilaire, A. Python, C. Rouch, M. Orosco and S. Nicolaidis
- 1331 Asymmetry of the interhemispheric visuomotor integration in callosal agenesis
M. Di Stefano and C. Salvadori
- 1337 The immune modulator Linomide prevents neuronal death in injured peripheral nerves of the mouse
P. A. R. Ekström, G. Hedlund, J. Karlsson and G. Andersson
- 1343 Modulation by GABA transmission in the substantia nigra compacta and reticulata of locomotor activity in rats exposed to high pressure
B. Kriem, B. Cagniard, C. Bouquet, J.-C. Rostain and J. H. Abraini
- 1349 A novel substance associated with gallamine-induced myoclonus
I. Ramzan, R. Goldsmith and W. Burke
- 1353 Seizures in rats treated with kainic acid induce Fos-like immunoreactivity in locus coeruleus
D. C. Silveira, Z. Liu, G. L. Holmes, D. L. Schomer and S. C. Schachter
- 1359 The effects of repeated alcohol exposure on the neurochemistry of the periadolescent nucleus accumbens septi
R. Montgomery Philpot and C. L. Kirstein
- 1365 Induction of NG108-15 cells differentiation by human bone marrow stromal cells
S.-H. Ho, L.-H. So, K.-O. Lai, N. Y. Ip and M.-F. Leung
- 1371 Phosphatidylcholine nigriventer toxins block tityustoxin-induced calcium influx in synaptosomes
D. M. Miranda, M. A. Romano-Silva, E. Kalapothakis, C. Ribeiro Diniz, M. N. Cordeiro, T. M. Santos, M. A. M. Prado and M. V. Gomez

Applicants: David J. Pinsky
U.S. Serial No.: 09/374,586
Filed: August 13, 1999
Group Art Unit: 1633

Contents continued overleaf

- 1375 TNF α induces a protein kinase C-dependent reduction in astroglial K⁺ conductance
H. Köller, N. Allert, D. Oel, G. Stoll and M. Siebler
- 1379 Abnormalities of Wnt signalling in schizophrenia – evidence for neurodevelopmental abnormality
D. Cotter, R. Kerwin, S. Al-Sarraj, J. P. Brion, A. Chadwick, S. Lovestone, B. Anderton and I. Everall
- 1385 (–)-Nicotine increases mRNA encoding G3PDH and the vesicular acetylcholine transporter *in vivo*
M. A. Prendergast and J. J. Buccafusco
- 1391 Phosmet induces up-regulation of surface levels of the cellular prion protein
I. Gordon, E. M. Abdulla, I. C. Campbell and S. A. Whatley
- 1397 Receptor-coupled phospholipase C and adenylyl cyclase function with different calcium pools in astrocytes
R. Balázs, S. Miller, Y. Chun and C. W. Cotman
- 1403 Primary structure of GAP-43 mRNA expressed in the spinal cord of ALS patients
M. Kage, A. Ikemoto, I. Akiguchi, J. Kimura, S. Matsumoto, H. Kimura and I. Tooyama
- 1407 Muscarinic toxin selective for m4 receptors impairs memory in the rat
D. Jerusalinsky, E. Kornisiuk, P. Alfaro, J. Quillfeldt, M. Alonso, E. R. Verde, C. Cerveñansky and A. Harvey
- 1413 Diversity of single potassium channels in isolated snail neurons
A. V. Sorkis, P. G. Kostyuk and E. A. Lukyanetz
- 1419 The effects of graded hypoxia on intraparenchymal arterioles in rat brain slices
M. Staunton, M. G. Dulitz, C. Fang, W. T. Schmeling, J. P. Kampine and N. E. Farber
- 1425 Microglial expression of the prion protein
D. R. Brown, A. Besinger, J. W. Herms and H. A. Kretzschmar
- 1431 Reduced kynurenine aminotransferase-I activity in SHR rats may be due to lack of KAT-1b activity
V. Kapoor, S. J. Thuruthyil and B. Human
- 1435 CEP-1347/KT7515, a JNK pathway inhibitor, supports the *in vitro* survival of chick embryonic neurons
G. D. Borasio, S. Horstmann, J. M. H. Anneser, N. T. Neff and M. A. Glicksman
- 1441 Intracisternal osteogenic protein-1 enhances functional recovery following focal stroke
T. Kawamata, J. Ren, T. C. K. Chan, M. Charette and S. P. Finklestein
- 1447 Hypoxic and hypoglycaemic changes of intracellular pH in cerebral cortical pyramidal neurones
T. Knöpfel, A. Tozzi, A. Pisani, P. Calabresi and G. Bernardi
- 1451 Increased expression of the TIAR protein in the hippocampus of Alzheimer patients
V. H. Oleana, A. Salehi and D. F. Swaab
- 1455 Rapid increase of NGF, BDNF and NT-3 mRNAs in inflamed bladder
D. Oddiah, P. Anand, S. B. McMahon and M. Rattray
- 1459 Differences in the kappa opioid receptor mRNA content in distinct brain regions of two inbred mice strains
A. Winkler and R. Spanagel
- 1465 Glucocorticoids alter recovery processes in the rat retina
I. Ábrahám, J. Pálhalmi, N. Szilágyi and G. Juhász
- 1469 Vestibular memory-contingent saccades involve somatosensory input from the body support
T. Mergner, G. Nasios and D. Anastasopoulos
- 1475 Evidence for an endogenous clock in the retina of rainbow trout: II. Circadian rhythmicity of serotonin metabolism
M. Zaunreiter, R. Brandstätter and A. Goldschmid
- 1481 Caspase-mediated cleavage is not required for the activity of presenilins in amyloidogenesis and NOTCH signaling
M. Brockhaus, J. Grünberg, S. Röhrig, H. Loetscher, N. Wittenburg, R. Baumeister, H. Jacobsen and C. Haass
- 1487 IFN- γ production of adult rat astrocytes triggered by TNF- α
B.-G. Xiao and H. Link
- 1491 Mannan-binding lectin in human serum, cerebrospinal fluid and brain tissue and its role in Alzheimer's disease
A.-S. Lanzrein, K. A. Jobst, S. Thiel, J. C. Jensenius, R. B. Sim, V. H. Perry and E. Sim
- 1497 Neuromagnetic fields preceding unilateral movements in dextrals and sinistrals
M. Taniguchi, T. Yoshimine, D. Cheyne, A. Kato, T. Kihara, H. Ninomiya, M. Hirata, N. Hirabuki, H. Nakamura and T. Hayakawa
- 1503 Reactive astrocytes express nitric oxide synthase in the spinal cord of transgenic mice expressing a human Cu/Zn SOD mutation
C. Ik Cha, J.-M. Kim, D. H. Shin, Y. S. Kim, J. Kim, M. E. Gurney and K. W. Lee
- 1507 Hippocampal atrophy is related to impaired memory, but not frontal functions in non-demented Parkinson's disease patients
P. Riekkinen Jr, K. Kejonen, M. P. Laakso, H. Soininen, K. Partanen and M. Riekkinen
- 1513 Neurogenic oedema and vasodilatation: effect of a selective neuronal NO inhibitor
P. K. Towler, G. S. Bennett, P. K. Moore and S. D. Brain
- 1519 Tacrine and donepezil attenuate the neurotoxic effect of A β (25–35) in rat PC12 cells
A.-L. Svensson and A. Nordberg

- 1523 Persistence of somatic and dendritic growth associated processes and induction of dendritic sprouting in motoneurons after neonatal axotomy in the rat
J. Dekkers and R. Navarrete
 - 1529 Mesencephalic THmRNA-reduced expression by blocking axonal transport with colchicine
O. Frain and V. Leviel
 - 1533 NGF and LIF both regulate galanin gene expression in primary DRG cultures
J. Corness, B. Stevens, R. D. Fields and T. Hökfelt
 - 1537 Hemispheric specialization for English and ASL: left invariance-right variability
D. Bavelier, D. Corina, P. Jezard, V. Clark, A. Karni, A. Lalwani, J. P. Rauschecker, A. Braun, R. Turner and H. J. Neville
 - 1543 Developmental changes in refractoriness of the neuromagnetic M100 in children
D. C. Rojas, J. R. Walker, J. L. Sheeder, P. D. Teale and M. L. Reite
 - 1549 Heat shock, but not the reactive state per se, induces increased expression of the small stress proteins hsp25 and α B-crystallin in glial cells in vitro
M. Brzyska, G. J. J. Stege, K. Renkawek and G. J. C. G. M. Bosman
 - 1553 Amyloid β -peptide(25-35) changes $[Ca^{2+}]$ in hippocampal neurons
H. S. Mogensen, D.M. Beatty, S. J. Morris and O. S. Jorgensen
 - 1559 Ecto-nucleotidases terminate purinergic signalling in the cochlear endolymphatic compartment
S. M. Vlajkovic, P. R. Thorne, G. D. Housley, D. J. B. Muñoz and I. S. Kendrick
 - 1567 Differential activation of dorsal basal ganglia during externally and self paced sequences of arm movements
V. Menon, G. H. Glover and A. Pfefferbaum
 - 1575 Modulation of neuropeptide Y overflow by leptin in the rat hypothalamus, cerebral cortex and medulla
J. Lee and M. J. Morris
 - 1581 The role of the left inferior temporal cortex for visual pattern discrimination - a PET study
R. Kawashima, K. Satoh, R. Goto, K. Inoue, M. Itoh and H. Fukuda
 - 1587 Electron spin resonance measure of brain antioxidant activity during ischemia/reperfusion
L. M. Katz, C. W. Callaway, V. E. Kagan and P. M. Kochanek
 - 1595 Purification of PASII/PMP22 - an extremely hydrophobic glycoprotein of PNS myelin membrane
J. Sedzik, Y. Kotake and K. Uyemura
 - 1601 The role of CRF₂ receptors in corticotropin-releasing factor- and urocortin-induced anorexia
G. N. Smagin, L. A. Howell, D. H. Ryan, E. B. De Souza and R. B. S. Harris
 - 1607 Two vocalization-related subregions in the midbrain periaqueductal gray of the guinea pig
S.-i. Kyuhou and H. Gemba
 - 1611 Transplantation of multipotent progenitors from the adult olfactory epithelium
B. J. Goldstein, H. Fang, S. L. Youngentob and J. E. Schwob
 - 1619 Ginseng improves strategic learning by normal and brain-damaged rats
R. Zhao and W. F. McDaniel
 - 1625 Intracellular Ca^{2+} and adaptation of voltage responses to light in Hermissenda photoreceptors
I. A. Muzzio, A. C. Talk and L. D. Matzel
 - 1633 Tetrahydroaminoacridine, a cholinesterase inhibitor, and d-cycloserine, a partial NMDA receptor-associated glycine site agonist, enhances acquisition of spatial navigation
P. Riekkinen Jr, S. Ikonen and M. Riekkinen
 - 1639 Localization of glutamate receptors in dorsal horn of rat spinal cord
K. K. L. Yung
 - 1645 Three time windows for amnesic effect of antibodies to cell adhesion molecule L1 in chicks
A. Tiunova, K. V. Anokhin, M. Schachner and S. P. R. Rose
 - 1649 Concept activation and coordination of activation procedure require two different networks
W. Krause, H. Gibbons and B. Schack
 - 1655 The hydroxyl radical scavenger Nicaraven inhibits glutamate release after spinal injury in rats
K. Yamamoto, T. Ishikawa, T. Sakabe, T. Taguchi, S. Kawai and M. Marsala
 - 1661 Neutrophin switching in spinal motoneurons of amyotrophic lateral sclerosis
T. Nishio, N. Sunohara and S. Furukawa
- Errata*
- 1667 The uterine environment enhances cognitive competence
V. H. Denenberg, B. J. Hoplight and L. E. Mobraaten
 - 1673 Neural activity in areas V1, V2 and V4 during free viewing of natural scenes compared to controlled viewing
J. L. Gallant, C. E. Connor, and D. C. Van Essen

THE vascular architecture of the brain of C57Black/6 and SV129 mice was studied following microvascular injection of carbon black stained latex. The dorsal brain surface was photographed to determine the number, diameter, and position of pial anastomotic vessels between the middle and anterior cerebral arteries. The mean number and diameter of anastomoses were not significantly different, but the line of anastomoses interconnecting the half way points of anastomotic vessels was located significantly closer to the midline in C57Black/6 mice, demonstrating that the middle cerebral artery had a larger vascular supplying territory than in SV129 mice. This explains the larger infarct volume previously reported in C57Black/6 mice, and raises concerns about the use of C57Black/6 and SV129 mice as parent strains for genetically modified animals in stroke research. *NeuroReport* 9: 1317-1319 © 1998 Rapid Science Ltd.

Key words: Anastomoses; Cerebral arteries; Cerebral vasculature; Mice; Mutant; Strain difference

Differences in the cerebrovascular anatomy of C57Black/6 and SV129 mice

Keiichiro Maeda, Ryuji Hata
and Konstantin-Alexander Hossmann^{CA}

Max-Planck-Institute for Neurological Research,
Department of Experimental Neurology,
Gleueler Str. 50, D-50931 Cologne, Germany

^{CA}Corresponding Author

Introduction

In recent years, genetically engineered animals have been used increasingly to investigate the molecular mechanisms of ischemic brain injury.¹⁻³ The most widely used parent strains for the production of mutants are C57Black/6 and SV129 mice, even though brain infarcts after permanent middle cerebral artery (MCA) occlusion are larger in the C57Black/6 than in the SV129 strain.⁴ This finding is disturbing, because differences in infarct volume after targeted gene mutation could be confused with differences in the genetic background of the two parent strains.

The most likely reason for strain differences in infarct volume is a difference in the vascular anatomy. The supplying territories of the major cerebral arteries are interconnected by Heubner's pial anastomoses which determine the efficiency of the collateral blood supply. Differences in the number and in the size of such anastomoses will, therefore, result in differences in the severity of the ischemic impact. Another anatomical factor could be a difference in the size of the vascular territory. In fact, the angioarchitecture is not strictly related to the gross anatomy of the brain and, therefore, may vary in different strains.

A straightforward way of investigating both the size of the vascular territory and the number and diameter of the anastomoses interconnecting these territories is the injection of the vascular system with

latex, as proposed by Coyle and Jokelainen.⁵ The resulting staining of the pial vessels facilitates the visualization of the peripheral branches of the supplying brain arteries and allows the precise identification and localization of the anastomotic vessels connecting these branches. Here, we demonstrate that the angioarchitecture of MCA does, in fact, differ in C57Black/6 and SV129 mice.

Materials and Methods

Experiments were carried out according to the NIH guidelines for the care and use of laboratory animals, and approved by the local authorities. Six male C57Black/6 mice and six male SV129 mice aged between 10 and 12 weeks were used (Harlan Winkelmann, Borcheln, Germany). Animals were housed under diurnal lighting conditions and allowed access to food and water *ad lib* before the experiment. Anesthesia was induced by 1.5% halothane and maintained with 1% halothane in 70% N₂O and 30% O₂. Rectal temperature was maintained at 36.5-37.0°C throughout the experiment, using an infrared lamp and a heating pad for feedback-controlled temperature stabilization (YSI, Yellow Springs, OH, USA).

The procedure used for visualization of the brain vasculature in mice was basically that described by Coyle and Jokelainen in rats.⁵ A lethal dose of papaverine hydrochloride (40-50 mg/kg, i.v. in sterile water) was injected to produce maximal vasodilation

and to minimize cerebrovascular resistance. The thoracic aorta was clipped at the level of diaphragm and cannulated with polyethylene tubing (internal diameter 0.58 mm, Portex, England). Warm (38°C), undiluted Vultex (a white latex; Chicago Latex Products no. 563) was mixed with a small amount of carbon black (10 μ l/g, Bokusai; Fueki, Tokyo, Japan) and was injected into the ascending aorta. The injection volume of latex was 0.4 ml, as determined in preliminary trials; the injection pressure was about 150 mmHg.

Thirty minutes after the injection, the animal was decapitated and the dorsal part of the skull and the dura were removed. To prevent deformation of the brain, the entire head was fixed in 10% formalin for 4 weeks before brain removal. Thereafter, the dorsal side of the brain was inspected under the operating microscope and photographed at $\times 20$ magnification. Preparations with unstained or ruptured pial vessels were excluded from the study.

Anastomoses on the dorsal surface of the hemispheres were localized by tracing the peripheral branches of the anterior cerebral artery (ACA) and the MCA to the anastomosis point, defined as the narrowest part of the vessel or half way between the nearest branching points of the ACA and the MCA branches, respectively.⁵ Adjacent anastomosis points were connected by the line of anastomoses,⁶ and the distance from the midline to the line of anastomoses was measured on photographs taken from the dorsal brain surface at coronal planes 2 mm, 4 mm and 6 mm from the frontal pole. The number of the anastomoses per hemisphere was counted, and the diameters of the two largest anastomoses in each hemisphere were measured using an image analyzer and NIH image 1.59 software (National Institutes of Health, Bethesda, MD, USA).

All values are given as means \pm s.d. The interstrain difference in the distance of the line of anastomoses from the midline was tested by one-way analysis of variance followed by Scheffé's *post hoc* analysis. Differences in the number and diameter of anastomoses between strains were tested for statistical significance using Mann-Whitney's U test.

Results

Figure 1 shows the dorsal aspect of the pial vasculature of a C57Black/6 mouse (left) and a SV129 mouse (right). In C57Black/6 mice the line of anastomoses between the ACA and the MCA was clearly closer to the midline than in SV129 mice. Quantitative evaluation of the distance between the line of anastomoses and the midline at three levels – 2 mm, 4 mm and 6 mm from the frontal pole –

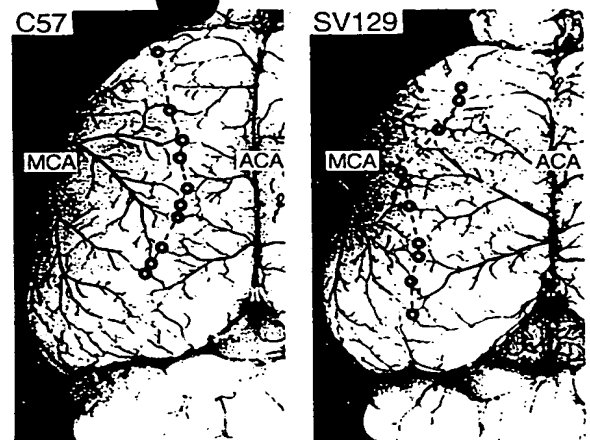


FIG. 1. Dorsal view of the cerebral hemisphere of C57Black/6 mice (left) and SV129 mice (right) after microvascular injection with carbon black stained latex. The points of anastomoses between the middle cerebral artery (MCA) and anterior cerebral artery (ACA) are marked with circles and connected by the line of anastomoses. Note the marked shift of the line of anastomoses to the midline in C57Black/6 mice.

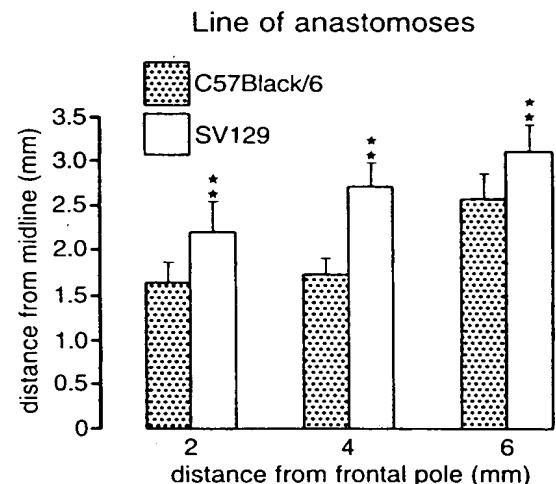


FIG. 2. Distance of the line of anastomoses from the midline in C57Black/6 mice (dotted bars) and SV129 mice (white bars) in three coronal planes, located 2 mm, 4 mm and 6 mm from the frontal pole. Note significantly smaller distance in the C57Black/6 mice, reflecting the larger MCA supplying territory in this strain (** $p < 0.01$).

revealed significant differences ($p < 0.01$) of up to 1 mm (Fig. 2).

In contrast to the position of the line of anastomoses, the number of anastomoses did not differ significantly in C57Black/6 mice (9.50 ± 1.51 per hemisphere) and SV129 mice (11.1 ± 2.50 per hemisphere). The diameter of anastomoses did not vary, either (C57Black/6: 26.6 ± 7.4 μ m; SV129: 23.4 ± 5.7 μ m).

Discussion

The architecture of the cerebral vascular system has been visualized by filling the microcirculation with low viscosity resin,⁷ Araldite F,⁸ gelatin mixed with India ink,⁹ or latex.⁵ Coyle and Jokelainen, who introduced the latex infusion method in the rat, infused a high dose of papaverine in order to produce maximal vasodilation and to minimize vascular resistance.⁵ We confirmed that this procedure also produced consistent cerebrovascular filling in mice but we found it difficult to detect small vascular branches because the white colour of latex produced too little contrast to the colour of the formalin-fixed brain tissue. We therefore modified the technique by staining the latex with carbon black. This modification allows easy demarcation even of the finest arterial anastomoses, and also facilitates the measurement of vascular diameter.

Using this method, marked differences of angioarchitecture were detected between C57Black/6 and SV129 mice. The supplying territory of the MCA was significantly larger in C57Black/6 mice, which readily explains the larger infarct volume observed in this strain.⁴ However, the volume of infarct also depends on other hemodynamic and molecular variables. Coyle and his co-workers reported that the diameter of anastomoses is an important factor in determining the supply to the occluded vascular territory.^{6,10,11} Our measurements, however, revealed that both the number and the diameter of papaverine-dilated anastomoses were identical in the two strains. Under ischemic conditions, C57Black/6 mice may even have an inherent hemodynamic advantage over the SV129 strain because the vasodilatory response to acetylcholine is more robust.¹² Another advantage of C57Black/6 mice could be their lower susceptibility to excitotoxicity, as observed after kainic acid-induced seizures.¹³ However, the investigation of hippocampal injury after global ischemia which is thought to result from excitotoxicity¹⁴ revealed just the opposite.¹² Thirty minutes bilateral carotid occlusion in C57Black/6 mice caused the same degree of cellular damage as 75 min of ischemia in SV129 mice, probably due to a hypoplastic posterior communicating artery in the former strain.¹² This example demonstrates that hemodynamic and molecular mechanisms of ischemic injury are intricately intermingled, and that it is impossible to predict ischemic susceptibility by consideration of any pathogenetic factors alone. The larger vascular territory supplied by the MCA in C57Black/6 mice is, therefore, a likely factor but not necessarily the only one responsible for the larger infarct volume after occlusion of this artery in this strain.⁴

The present demonstration of the angioarchitectural differences in C57Black/6 and SV129 strains adds to the growing concern over the use of genetically engineered mice for the study of ischemic injury. In most of these investigations, embryonic stem cells are derived from SV129 mice, and after gene targeting the resultant chimeric mice are mated with C57Black/6 mice.¹⁵ The offspring, therefore, carry both C57Black/6 and SV129 genes. According to the theory of genetic linkage, pseudo-correlations may evolve if the targeted gene locus is located close to the gene related to cerebral arterial architecture. It is, therefore, mandatory to confirm that independent variables, such as differences in the vascular architecture, do not interfere with the result of gene targeting. An alternative approach would be backcrossing with a single parent strain for at least 12 generations to ensure homogeneity of genetic background.¹⁵ However, as pointed out by Fujii *et al.*,¹² such an approach is time-consuming and expensive. Visualization of the vascular supplying territory is a much simpler and more straightforward method of detecting or refuting the existence of such interactions, and is strongly recommended.

Conclusions

The supplying territory of the middle cerebral artery is significantly larger in C57Black/6 mice than in the SV129 strain. This explains the previously documented difference in infarct volume in C57Black/6 and SV129 mice and adds to the growing concern about the use of these animals as parent strains for genetically engineered mutants in stroke research.

References

1. Crumrine R, Thomas A and Morgan P. *J Cereb Blood Flow Metab* **14**, 887-891 (1994).
2. Kamii H, Kinouchi H, Sharp FR *et al.* *J Cereb Blood Flow Metab* **14**, 478-486 (1994).
3. Hara H, Huang PL, Panahian N *et al.* *J Cereb Blood Flow Metab* **16**, 605-611 (1996).
4. Connolly ES, Winfree CJ, Stern DM *et al.* *Neurosurgery* **38**, 523-532 (1996).
5. Coyle P and Jokelainen P. *Anat Rec* **203**, 397-404 (1982).
6. Coyle P. *Stroke* **18**, 1133-1140 (1987).
7. Sbarbati A, Pietra C, Baldassarri AM *et al.* *Acta Neuropathol* **92**, 56-63 (1996).
8. van der Zwan A, Hillen B, Tulleken CAF *et al.* *J Neurosurg* **77**, 927-940 (1992).
9. Duvernoy HM, Delon S and Vannson JL. *Brain Res Bull* **7**, 519-579 (1981).
10. Coyle P. *Anat Rec* **218**, 40-44 (1987).
11. Coyle P and Feng X. *Stroke* **24**, 705-710 (1993).
12. Fujii M, Hara H, Meng W *et al.* *Stroke* **28**, 1805-1811 (1997).
13. Schauwecker PE and Steward O. *Proc Natl Acad Sci USA* **94**, 4103-4108 (1997).
14. Juurlink BH and Sweeney ML. *Neurosci Biobehav Rev* **21**, 121-128 (1997).
15. Gerlai R. *Trends Neurosci* **19**, 177-181 (1996).

Received 16 February 1998;
accepted 19 February 1998